Author's response to Review RC1 by Emmanuel Dekemper

We are very gratefully acknowledging the comments of Emmanuel Dekemper. The comments are highly helpful in both, in enhancing the clarity of the presented technique and model.

For clarity we answer the specific comments directly (bold printed). The reviewer comments are set in italic font, the authors' responses in normal font. We added a new Figure (Fig. 2) and included a SO2 flux calculation at the end of Section 3.3 and in Section 4. In several places throughout the manuscript we modified and extended sentences yielding minor changes to the manuscript.

1.1 The abstract

Reviewer's comment: Although the abstract is a good summary of the manuscript (high level description of the instrument concept, and the experimental results achieved), I think it is slightly ex-aggerating the demonstrated capabilities of the instrument. For instance, it is claimed that the instrument does the job for SO2, BrO, and NO2, whereas only the first species is addressed. I understand that the prototype was designed to correlate with the SO2 structures, but therefore, at least a theoretical simulation of performance for the other species should have been presented. In absence of this, the BrO and NO2 capabilities should only be referred to as potential future applications. The same goes for the statement that the instrument allows to determine gas fluxes, while this aspect is also not discussed in the paper. The factual performance of the prototype is also a bit misleading: the claimed integration time of 1s is, as far as I could understand, the integration time of a single image, not yet the temporal resolution of the geophysical product (presumably closer to 5 seconds) as it seems currently suggested. Hence, I would recommend to rework a bit the abstract such that undemonstrated, though potentially achievable goals are not presented as conclusions of the work.

Author's response:

- Indeed, we did only present imaging measurement results of volcanic SO_2 emissions. Of course, the FPI employed for that was specifically designed to correlate with SO_2. However, the camera prototype itself was not solely implemented for SO_2. Replacing the BPF and the FPI, by one that is designed for BrO or NO_2 the camera can be used for measuring further gas species. Within this manuscript we did in fact not present theoretical simulation of the performance for gases other than SO_2 since these were already presented in a former manuscript (Kuhn et al. 2019). We will therefore change the claim to be able to measure BrO and NO2 to future applications.

  We changed the sentence (submitted manuscript lines: 4 - 6):
  "Matching the FPIs distinct, periodic transmission features to the characteristic differential absorption structures of the investigated trace gas allows to measure differential atmospheric column density (CD) distributions of numerous trace gases, e.g. sulphur dioxide (SO_2), bromine monoxide (BrO), or nitrogen dioxide (NO_2), with high spatial and temporal resolution."

To (revised manuscript lines: 3 - 6):
“Matching the FPIs distinct, periodic transmission features to the characteristic differential absorption structures of the investigated trace gas allows to measure differential atmospheric column density (CD) distributions of numerous trace gases with high spatial and temporal resolution. Here we demonstrate measurements of sulphur dioxide (SO_2) while earlier model calculations show that bromine monoxide (BrO) and nitrogen dioxide (NO_2) are also possible.”

- Further, we stated that we can determine gas fluxes since it is usually possible to retrieve fluxes from an image time series with sufficient high spatial resolution. However, the viewing geometry on the day of measurement was quite unfavourable as the plume propagation direction and field of view direction only had low inclination of 19° in contrast to ideal condition with a plume perpendicular to the viewing direction. Also, the fact that the plume was partly covered by the crater flank only allows to calculate a lower limit to the actual gas flux. Nonetheless, we now include a flux calculation in the article and discussing the unfavourable conditions for this particular example, which lead to a rather high measurement error but is showing the capability of IFPICS to determine fluxes.

  We added the sentences (revised manuscript lines: 238 - 259):
  “After the proof of concept, showing the capability of IFPICS to determine SO_2 CD images it is possible to determine fluxes from a CD image time series. Especially, if the series allows to trace back individual features in consecutively recorded images it can be used to directly determine the plume velocity using the approach of cross-correlation (e.g. McGonigle et al., 2005; Mori and Burton, 2006; Dekemper et al., 2016) or optical flow algorithms (e.g. Kern et al., 2015b) and to determine the plume propagation direction (e.g. Klein et al., 2017). However, the viewing geometry on the day of our measurement was unfavourable as it was not possible to reach another measurement location due to a lack in infrastructure. The plume propagation direction and central line of sight show an inclination of 19° only, resulting in high pixel contortions, especially for pixel close to the edges of the FOV. Further, significant parts of the plume are covered by the crater flank due to its propagation direction. For the sake of completeness, we would like to give a rough estimate on the SO_2 flux obtained from our data.
  The SO_2 flux Φ_{SO2} is determined by integrating the SO_2 CD along a transect through the volcanic plume and subsequent multiplication by the wind velocity perpendicular to the FOV direction, however due to the viewing geometry issues we will use external wind data (direction: 5°; velocity $v_{wind} \approx 6$ m s^{-1} (data from UWYO)) for the calculation. As the camera pixel size is finite the integral is replaced by a discrete summation over the pixel n

  $$\Phi_{SO2} = v_{\perp} \sum_n S_{SO2;n} \cdot h_n$$

  including the perpendicular wind velocity $v_{\perp}$, the SO2 CD $S_{SO2;n}$ and the pixel extent h_n. The perpendicular wind velocity can directly be calculated from geometric considerations (see Fig. 5, (a)), accounting to $v_{\perp} \approx sin(19°)\, v_{wind} \approx 2$ m s^{-1}. To determine the pixel extent the distance between the volcanic plume and the location of measurement is required. In the centre of the FOV this

distance is ≈3500m yielding h_n ≈2,7 m. To keep the impact of pixel contortions low the plume transect is located centrally in the FOV at column 250 and ranging from rows n = 230 to 330. Using these quantities, we retrieve a mean SO_2 mass flux for the measurement of Φ_{SO2} = (84±11) t d^{-1} for the investigated plume of the South East crater. Nevertheless, the flux should be regarded as lower limit, since the plume was covered by crater flank to an unknown extent."

We changed & relocated the sentence (submitted manuscript lines: 231 - 233):
"Also, the imaging technique lends itself to the determination of gas fluxes. For instance, the wind velocity and also the angle between the observation direction and plume propagation direction can be determined from the image series."

To (revised manuscript lines: 266 - 271):
"Also, the imaging technique lends itself to the determination of gas fluxes and we obtained an SO2 mass flux of Φ_{SO2} = (84±11) t d^{-1} for Mt. Etna's South East crater plume. However, due to unfavourable conditions in the viewing geometry the retrieved flux should be treated as a lower limit. In general, it is possible to apply optical flow algorithms on image series acquired under more ideal viewing geometry conditions (e.g. Kern et al., 2015b). These allow to determine the plume velocity and angle between the observation direction and plume propagation direction in order to retrieve accurate so2 fluxes (e.g. Klein et al., 2017)."

- We added the total time required for the acquisition of a pair of images, including tilting, and saving the images, which was 5.5 seconds for the used prototype setup. In further instrument versions, image readout and motor movement are negligible compared to the exposure time of 1 s.

  We further changed the sentence (submitted manuscript lines: 9 - 11):
  "In a field campaign, we recorded the temporal CD evolution of SO2 in the volcanic plume of Mt. Etna with an integration time of 1 s and 400x400 pixels spatial resolution. The first IFPICS prototype can reach a detection limit of 2,1×10^{17} molec cm^{-2} s^{-1}, which is comparable to traditional and much less selective volcanic SO_2 imaging techniques."

  To (revised manuscript lines: 9 - 14):
  "In a field campaign, we recorded the temporal CD evolution of SO_2 in the volcanic plume of Mt. Etna with an exposure time of 1 s per image and 400 x 400 pixel spatial resolution. The temporal resolution of the time series was limited by the available non-ideal prototype hardware to about 5.5 s. Nevertheless, a detection limit of 2,1×10^{17} molec cm^{-2} could be reached, which is comparable to traditional and much less selective volcanic SO2 imaging techniques."

1.2 The instrumental model

Reviewer's comment: The mathematics describing the measurements have been carefully developed, and the reader will appreciate the author's will to integrate all the meaningful aspects of the model (in particular the splitting of the instrument transfer function into different multiplicative terms). However, I have two remarks regarding this section:

1. *Less experienced readers might be lost in this section because it lacks a drawing representing the light paths involved. Supporting the mathematical description with a figure showing that eq.(2) refers to the light path originating from the Sun and going up to the point of scattering into the instrument line of sight would already be helpful. Having two rays illustrating the difference between Ii, and I0,i would also be appreciated.*

2. *Recalling the reader about the fundamental FPI equation is valuable. However, eq.(7) appears to be a step too far, especially that the weighting function term N remains mysterious at the end. I believe that the discussion on the effective transmission spectrum of the FPI is an important point. But because the reader will anyway not be able to reproduce your model (because of the undetermined term N), it is better to illustrate the effect of increasing the acceptance angle (or the tilt angle) on the FPI transmission with the help of a figure (a bit like fig.(1),but emphasizing the change of T_{FPI} as a function of these angles). Also, I found it not so clearly explained that the way the comb of the FPI is shifted (to go from setting A to B and back) is by rotating the FPI axis. A few words about the different means of performing this shift with nowadays FPI technologies (e.g. MEMS, piezo), and the trade off which led to the selection of the tilting approach would be appreciated.*

Author's response:

Point 1: This is a good suggestion. We extended the introduction of the mathematical model by a graphical representation, which is now Fig. 2.

> "A 2D UV-sensitive CMOS sensor (SCM2020-UV provided by *EHD imaging*) is used to acquire images."

We included a new figure; Fig. 2:

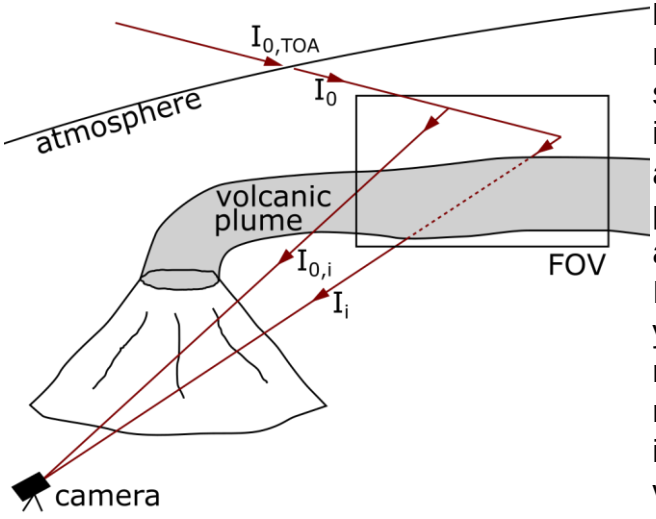

Figure 2. Schematic of the IFPICS measurement geometry including the simulated radiances used in the instrument model. The incident top of atmosphere (TOA) radiation $I_{0,TOA}$ is propagating through the atmosphere and is potentially scattered into the IFPICS camera field of view (FOV) yielding the scattered skylight radiance I_0. The camera records radiation in the respective FPI settings i = A and B that either traverses the volcanic plume I_i or originates from a plume free area within the FOV $I_{0,i}$.

Point 2: We had many thoughts about how detailed we should present our applied model. We tried to make it as detailed as possible and the representation of the final equation (Eq. (7)) was frequently discussed among the authors. Due to its high complexity, requiring three case analyses, all resulting in a different function, we ultimately only showed a more general equation trying to emphasize the basic principle. The quantity *N* representing the weighting and is given by the integral in Eq. 7 excluding the integrand $T_{FPI,i}$. We will include a description in the revised version of the manuscript.
Thanks for the comment concerning the shift of the FPI comb. We will emphasize this point in both, the introduction of the model, and in the description of the prototype setup. Further we will add a description to the manuscript why we use a tilting approach.

We added the sentences (revised manuscript lines: 104 - 107):
"The FPI used in this work is static and air-spaced, meaning *d*, *n*, and *R* are fixed. Hence, the incidence angle α_i is the exclusive free parameter available to tune the FPIs transmission spectrum $T_{FPI;i}$ between settings *i* = A and *i* = B respectively. The change in α_i is achieved by tilting the FPI optical axis with respect to the imaging optical axis (see Section 2.2)."

We changed the sentence (submitted manuscript lines: 107 - 108):
"Thereby, $N(\gamma(\alpha_i,\omega_c))$ denotes the weighting function, ϑ the polar angle and φ the azimuth angle of the spherical integration within boundaries defined by the tilted cone shaped light beams."

To (revised manuscript lines: 115 - 117):
"Thereby, $N(\gamma(\alpha_i,\omega_c))$ denotes the weighting function with $N(\gamma(\alpha_i,\omega_c)) = \iint \sin\vartheta \, d\vartheta \, d\varphi$ given by the integral in Eq. 7 excluding the integrand $T_{FPI,I}$ itself, ϑ the polar angle and φ the azimuth angle of the spherical integration within boundaries defined by the tilted cone shaped light beams."

We changed and extended the sentence (submitted manuscript lines: 125 - 127):
The static air-spaced FPI (*d*, *n* and *R* fixed, provided by *SLS Optics Ltd*.) can be tilted within the parallelised light path in order to tune its spectral transmission T^{eff}_{FPI} between setting A and B via variation of the incidence angle α (see Section 2.1).

To (revised manuscript lines: 135 - 138):
The FPI is the central optical element of the IFPICS prototype and is implemented as static air-spaced etalon with fixed *d, n*, and *R* (provided by *SLS Optics Ltd*.). The mirrors are separated using ultra low expansion glass spacers to maintain a constant mirror separation *d* and parallelism over the large clear aperture of 20 mm even under highly variable environmental conditions. In order to tune the spectral transmission T^{eff}_{FPI} between setting A and B a variation of the incidence angle α is applied.

We added the sentence (revised manuscript lines: 141 - 143):
We favour the approach of tilting the FPI over changing internal physical properties like, e.g. the mirror separation *d* by piezoelectric actuators, as it keeps simplicity, robustness, and accuracy high for measurements under non-laboratory conditions.

1.3 Minor comments

- *Reviewer's comment: p.2,l.26: The NO2 camera, presented in Dekemper et al. 2016, has a spectral resolution of 0.6nm at 440nm... The statement that native spectral imagers have a "strongly reduced spectral resolution" is therefore not correct. It is not because the classical filter-based SO2 cameras have a poor spectral resolution that all other spectral imagers have the same drawback, especially when the filter technology is completely different.*

  Author's response:

  We changed and extended the sentence (submitted manuscript lines: 24 - 30):
  "A third approach applies a small number of (typically two) wavelength channels by using wavelength selective optical elements for the entire image frame, thereby usually strongly reducing the spectral resolution (e.g. Mori and Burton, 2006; Dekemper et al., 2016). The high spectral resolution of the first two, spectrograph based approaches allows the accurate and simultaneous identification of several trace gases, however, the light throughput and the scanning process severely limit the temporal resolution. The third approach can be quite fast, the trace gas selectivity, however, strongly depends on the correlation of trace gas absorption with the wavelength selective elements and usually is rather marginal."

  To (revised manuscript lines: 26 - 34):
  "The high spectral resolution of the spectrograph based techniques allows the accurate and simultaneous identification of several trace gases, however, the light throughput and the scanning process severely limit the temporal resolution. A third approach applies tunable filters to resolve the trace gas spectral features, e.g. acousto-optical tunable filter (Dekemper et al., 2016), as wavelength selective elements for an entire image frame. The application of tunable filters can have high spectral resolution and hence high trace gas selectivity, however, due to limited light throughput the temporal resolution lies in the order of minutes. A fourth imaging technique uses a small number (typically two) wavelength channels selected by static filters, e.g. interference filters (Mori and Burton, 2006). This approach can be quite fast with a temporal resolution in the order of seconds, the trace gas selectivity, however, strongly depends on the correlation of trace gas absorption with the wavelength selective elements and usually is rather marginal."

- *Reviewer's comment: I was wondering if the tilting of the FPI in order to go from setting A to B was introducing a shift of the respective images onto the detector? Is there a re-alignment step needed in the pre-processing of the data? If yes, then this is worth a couple of sentences addressing this aspect.*

  Author's response: Yes, indeed the tilting is inducing a linear shift of the respective images A and B on the detector. Therefore, a realignment step for the processing is performed accounting for a shift of 6 pixels. In the revised version we will address this point in Section 2.2 and 3.1.

We added the sentence (revised manuscript lines: 143 - 145):
“However it need to be considered, that the tilting of the FPI will generate a linear shift between the respective images acquired in setting A and B, requiring an alignment in the evaluation process.”

We added the sentence (revised manuscript lines: 166 - 167):
“The tilt of the FPI generates a linear shift between the recorded on-band and off-band images on the detector and accounts for 6 pixel using tilt angles α_i. This shift needs to be corrected before cross evaluating images recorded in setting A and B.”

- *Reviewer’s comment: Section 3.2: Your forward model uses a geometric air mass factor to estimate the SCD of O3. The model was validated for a relatively small SZA with the two gas cells. However, your field measurements were performed with a much larger SZA of almost 80°. Don’t you expect a bias coming from the geometric AMF in that circumstances?*

  Author’s response: Yes indeed, large SZA can impact the calibration function retrieved by the instrument model. We geometrically recalculated the O_3 AMF assuming a homogeneous spherical shell of O_3 within a spherical nonrefracting atmosphere. For an SZA of 78° the retrieved change in the O_3 AMF is -7.5% translating to a sensitivity increase of +3.6% of the calculated calibration function. As the bias is rather small, we will not include the correction in model applied in this work. We will extend our model by a more general AMF calculation in future studies.

- *Reviewer’s comment: p.10,l.203: How did you estimate the background SO2? Your method relies on using the background signal in order to determine the CD in the plume. Which I0 did you use for the determination of the background SO2?*

  Author’s response: The SO_2 background signal has no significant impact on the measurement. A plume-free region within the measurement image is used to calculate the differential SO_2 signal induced by the plume (see: revised manuscript lines: 226 - 230). The model is not impacted by the atmospheric SO_2 background, since its absorption does not significantly impact the shape of the solar spectrum in the measurement wavelength range.

1.4 Typos

- p.4,l.80: stratosperhic -> stratospheric
  corrected as proposed

- p.7,l.145: describe -> described
  corrected as proposed

- p.7,l.151: add a comma after "model"
  corrected as proposed

- p.7,l.154: add a comma after "quality"

corrected as proposed

- p.7,l.157: including -> include
  corrected as proposed

- p.8,l.173: add a comma after the first "model"
  corrected as proposed

- On several occasions, the form "I. e." is used at the beginning of a sentence (like on p.8, line 177). I don't understand this abbreviation.
  We changed the abbreviation "I.e." occurring at the beginning of the sentences either into "In other words" or "That is to say".

- p.8,l.179: remove the comma after "Note"
  corrected as proposed

- p.10,l.199: start a new paragraph with "An evaluated ..."
  corrected as proposed

- p.11,l.229: "increases selectivity" -> "increases the selectivity"
  corrected as proposed